Proc. Natl. Acad. Sci. USA
Vol. 90, pp. 6493–6497, July 1993
Biochemistry

Kinetic control of Ca(II) signaling: Tuning the ion dissociation rates of EF-hand Ca(II) binding sites

(troponin C/parvalbumin/calmodulin/*Escherichia coli* galactose binding protein/site-directed mutagenesis)

MICHAEL RENNER, MARK A. DANIELSON, AND JOSEPH J. FALKE*

Department of Chemistry and Biochemistry, University of Colorado, Boulder, CO 80309-0215

Communicated by Thomas R. Cech, March 25, 1993

ABSTRACT **EF-hand Ca(II) binding sites share a conserved architecture and are prevalent in Ca(II) signaling pathways. The ion binding kinetics of these sites are carefully tuned to provide the physiologically appropriate activation and inactivation time scales. Here we examine kinetic tuning by the side chain at the ninth position of the EF-loop. A model is proposed in which both the size and charge of the side chain contribute to kinetic tuning. To test this model, the ninth loop position of the EF-hand-like site in the *Escherichia coli* D-galactose binding protein has been engineered and the Tb(III) dissociation kinetics of the resulting sites have been analyzed. Substitutions at this position are observed to generate up to 10^4-fold changes in Tb(III) dissociation rates, with little effect on Tb(III) affinity. Furthermore, the observed pattern of rate changes confirm the model's predictions; long side chains at the ninth loop position yield slow dissociation kinetics as predicted for a steric block, whereas acidic side chains yield slow dissociation kinetics as expected for an electrostatic barrier.**

The EF-hand Ca(II) binding motif is widespread in eukaryotic Ca(II) signaling systems where it is used for Ca(II) activation, buffering, and structural stabilization (for reviews, see refs. 1–6). At least 276 putative EF-hand Ca(II) sites have been identified to date by sequence homology (7), and the crystal structures of 24 EF-hand sites are known (8–13). Each EF-hand site utilizes a 12-residue loop to provide seven oxygens for Ca(II) binding; invariably these oxygens surround the bound ion in a pentagonal bipyramidal coordination geometry (Table 1 and Fig. 1) (8).

Significant progress has been made in delineating cellular EF-hand Ca(II) signaling networks (1–6), yet much remains to be learned about the control of their kinetics. In a given pathway, both the activation and inactivation kinetics must be optimized to generate the appropriate response time and duration, particularly in pathways regulated by a temporal sequence of Ca(II) binding to multiple EF-hand proteins. For instance, the contraction signal of skeletal muscle (21, 22) begins with a Ca(II) flux from the sarcoplasmic reticulum. The incoming Ca(II) binds first to troponin C, the trigger component of the tropomyosin complex. Then, after a brief lag phase, the bound Ca(II) population shifts to parvalbumin, which serves to sequester Ca(II) and inactivate the contraction signal, until the Ca(II) is returned to the sarcoplasmic reticulum.

This ordered flow of Ca(II) between the EF-hand sites of troponin C and parvalbumin is provided by differences in their ion binding kinetics, specificities, and affinities. Troponin C possesses two fast-activation sites exhibiting high Ca(II) specificity and relatively short halftimes for Ca(II) loading and unloading, such that for each two-step event, the overall time scale is $t_{1/2} < 10$ msec (23, 24). In contrast, the two slow-buffering sites of parvalbumin are less Ca(II)-specific and are initially saturated with Mg(II). The slow dissociation of Mg(II) from these sites provides the needed lag phase of $t_{1/2} \approx 1$ sec prior to Ca(II) binding (22, 25). [Parvalbumin also exhibits slow dissociation for other multivalent cations, indicating that slow dissociation kinetics are a characteristic feature of its cooperative binding sites (25).] Finally, the Ca(II) affinity of parvalbumin ($K_d \approx 10$ nM) is significantly greater than that of the troponin C activation sites ($K_d \approx 3$ μM), providing a net flow of Ca(II) from troponin C to parvalbumin during the approach to equilibrium (23, 26).

Previous studies have begun to elucidate the molecular mechanisms underlying affinity (27) and specificity (28–32) tuning; and 4-fold kinetic tuning has been accomplished by varying surface charge near an EF-hand site (33). However, most of the 10^3-fold range of Ca(II) dissociation rates from EF-hand sites (22, 25, 34) remain to be explained in terms of structural features. The present study begins by comparing the tertiary and primary structures of fast and slow EF-hand Ca(II) sites to identify residues that might be involved in kinetic tuning. Subsequently, a candidate residue is tested in the experimentally accessible EF-hand-like site of the *Escherichia coli* galactose binding protein. Since only the Ca(II)-occupied structures of EF-hand sites have been well-studied, the focus is on metal ion dissociation rather than association. The results suggest that the ninth EF-loop position plays a key role in kinetic tuning and, moreover, that kinetics can be tuned independently of affinity.

METHODS

Engineering the Ca(II) Binding Site of the *E. coli* Galactose Binding Protein. Plasmid pSF5 bearing the gene for galactose binding protein was engineered by oligonucleotide-directed mutagenesis as described (31). The resulting wild-type and engineered genes were expressed in *E. coli* and the protein was purified by standard procedures (31, 35). Bound metal ions were removed by dialysis (31, 35, 36); the final dialysis buffer was 100 mM KCl [Ca(II)-electrode grade, Orion]/10 mM Pipes·KOH, pH 6.0.

Tb(III) Dissociation Measurements. To quantitate Tb(III) dissociation, the binding protein at 2.5 μM was allowed to equilibrate overnight at 25°C with 25 μM $TbCl_3$ in final buffer. Bound Tb(III) fluorescence was selectively monitored by steady-state energy transfer from nearby Trp-127 (λ_{ex} = 292 nm; λ_{em} = 543 nm; bandwidths = 4 nm) (31, 35, 36); the dissociation time course was triggered by the addition of 0.3 mM EDTA. For the Asn-142 site, it was necessary to initiate the time course by stopped-flow rapid mixing, yielding the same final ionic parameters.

RESULTS

A Model for Kinetic Tuning. Examination of the known EF-hand crystal structures reveals a specific side-chain po-

The publication costs of this article were defrayed in part by page charge payment. This article must therefore be hereby marked "*advertisement*" in accordance with 18 U.S.C. §1734 solely to indicate this fact.

*To whom reprint requests should be addressed.

Table 1. Summary of coordinating residues in 276 EF-hand Ca(II) binding sites

Site	Residue 1 (side chain)	2	3 (side chain)	4	5 (side chain)	6	7 (backbone)	8	9 (side chain or H_2O)	10, 11	12 (side chain)
Consensus (276 seqs)	**Asp** (99%, 273)		**Asp** (75%, 207)		**Asp** (57%, 158)		**−C=O** (100%)		**Asp** (33%, 92)		**Glu** (91%, 252)
Parvalbumin site 1 (22 seqs)	Asp (22)		Asp (22)		Ser (22)		Phe (17) Tyr (5)		Glu (22)		Glu (22)
Troponin C, calmodulin sites 1–4 (129 seqs)	Asp (128) Asn (1)		Asp (106) Asn (23)		Asp (74) Asn (37) Ser (13) Gly (5)		Thr (50) Gln (20) Tyr (19) Phe (10) Arg (8) Asp (5) Asn (3) Leu (3) Cys (3) Ser (2) His (2) Lys (1) Ala (1) Val (1) Gly (1)		Asp (54) Ser (28) Thr (24) Asn (22) Glu (1)*		Glu (129) Gln (1)
Other sites (125 seqs)	Asp (123) Glu (1) Tyr (1)		Asp (79) Asn (31) Glu (13) Ser (2)		Asp (84) Asn (22) Ser (15) Glu (2) Gln (1) Thr (1)		Lys (30) Glu (15) Thr (15) Phe (13) Tyr (9) Ser (8) Val (7) Ala (5) Ile (4) Asp (4) Arg (3) Met (3) Leu (3) Asn (2) Gln (2) Gly (1) Pro (1)		Asp (38) Gly (27) Ser (21) Thr (12) Met (11) Glu (6) Gln (2) Arg (2) Asn (2) Cys (1) Leu (1) Val (1) Ala (1)		Glu (101) Asp (17) Val (4) Asn (2) Leu (1)

Shown are the 12 positions of the EF-hand Ca(II) binding loop. The type of coordination provided by each of the six coordinating positions is indicated, and the consensus residues most commonly used for coordination are in boldface type. Also summarized are the nonconsensus residues observed at these positions. The number of occurrences of each residue is indicated in parentheses. Data were compiled from 276 EF-loop sequences (7). At the ninth position, Glu or Gln provides direct coordination, whereas shorter side chains yield coordination by solvent. seqs, Sequences.

*From the *Saccharomyces cerevisiae* CMD1 protein, which lacks an essential Ca(II) signaling function (14, 15).

sition where kinetic tuning might occur and suggests a model in which tuning is partly controlled by steric factors (Figs. 1 and 2). In each structure, the shortest path connecting the bound Ca(II) to bulk solvent is partially or completely blocked by the axial ninth side chain of the EF-loop. Further examination of these structures reveals two distinct classes of axial coordination. (*i*) When the side chain is Glu or Gln, the side chain carboxyl oxygen provides direct coordination to the Ca(II) (4 examples, refs. 8–13, 16), thereby yielding the maximum steric hindrance to dissociation, as summarized in Fig. 1*A*. (*ii*) In contrast, shorter residues at the ninth loop position never provide direct coordination (20 examples, refs. 8–13, 16); instead the axial ligand is a water oxygen, often stabilized by outer-sphere coordination to the side chain as illustrated in Fig. 1*B* (16). Such axial coordination by solvent is proposed to generate less steric hindrance to dissociation and may even provide a dissociation channel leading to the bulk solvent (Figs. 1 and 2).

The information provided by EF-hand primary structures (Table 1) is consistent with the steric component of the model and suggests an electrostatic component of kinetic tuning as well. The EF-hand family with the slowest metal dissociation kinetics (25), namely, the parvalbumins with 22-member sequences, possesses a perfectly conserved Glu at the ninth loop position of their N-terminal site (Table 1 and ref. 7). The slow dissociation kinetics of these proteins is proposed to stem in part from steric hindrance by direct Glu coordination and in part from an electrostatic barrier to dissociation provided by the Glu charge. In contrast, the rapid EF-hand sites (23, 24, 34) of troponin C and calmodulin possess neither Glu nor Gln at the ninth loop position in 128 of the 129 described sequences (Table 1 and ref. 7). [The sole exception is the Glu in site 2 of the *Saccharomyces cerevisiae* CMD1 protein (14), an atypical calmodulin that lacks an essential Ca(II) signaling function (15).] Instead the rapid sites utilize shorter side chains including Asn, Ser, and Asp (Table 1 and ref. 7). This lack of sequence overlap between rapid and slow sites is unique to the ninth loop position; at the other five coordinating positions, side chains are shared extensively between the two kinetic classes. Interestingly, for the rapid sites, the ninth loop position also exhibits the greatest sequence variability, consistent with its proposed role in tuning.

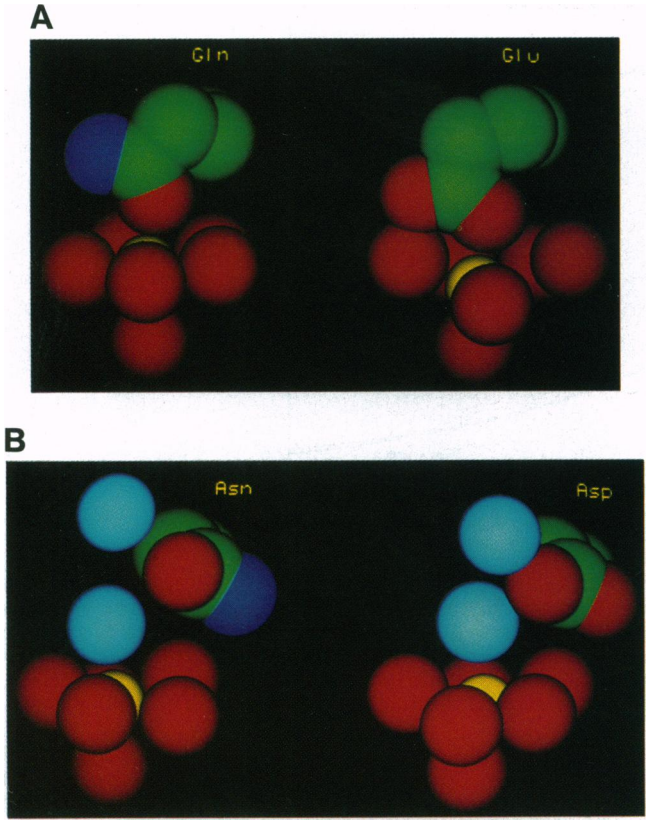

FIG. 1. Axial Ca(II) coordination at the ninth position of the EF-loop. Four representative sites illustrating the two types of axial coordination associated with the ninth EF-loop position [−X in the octahedral designation (16)]. The sites are oriented such that the nearest solvent interface is reached by vertical migration of the ion. Shown for each site is the bound Ca(II) (yellow atom) surrounded by the pentagonal bipyramidal array of coordinating oxygens (red atoms). Highlighted is the side chain of the ninth loop position (carbon is green and nitrogen is blue). (*A*) Gln and Glu side chains provide direct inner sphere Ca(II) coordination. To the left is the Ca(II) site of the *E. coli* galactose binding protein (17); to the right is site II of parvalbumin (18). (*B*) Asn and Asp side chains stabilize inner sphere coordination by a water oxygen (aqua atom). Also shown is the second most proximal water oxygen. To the left is site IV of calmodulin (19); to the right is site III of troponin C (20).

Testing the Kinetic Tuning Model by Engineering the Ninth Position of the Loop. The steric and electrostatic tuning model makes simple predictions that can be tested by engineering the ninth loop position of a representative EF-hand site and then quantitating the effects on metal ion dissociation. The *E. coli* periplasmic galactose binding protein, which utilizes Ca(II) binding for structural stabilization, possesses a single Ca(II) binding site with an EF-hand-like structure as discussed in detail (17). Two features of this site make it useful for quantitative measurements: (*i*) it possesses the binding properties of a simple independent site lacking the complications of cooperative multisite systems and (*ii*) it provides Trp-127 within 5 Å of the bound ion for sensitive fluorescence detection of metal binding (35, 36). The present study employs four versions of the site (31): the wild-type site that possesses Gln at the ninth loop position [Q142(WT)] and the three most conservatively engineered sites possessing Glu, Asn, or Asp at this position (Q142E, Q142N, or Q142D, respectively).

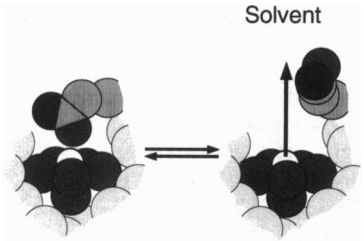

FIG. 2. Schematic model for Ca(II) dissociation from an EF-hand Ca(II) site. Shown are the seven coordinating oxygens (darkly shaded spheres) surrounding the central Ca(II) atom (small open sphere), as well as the axial side chain of the ninth loop position, which is proposed to tune the dissociation rate (explicitly shown at the top of the figure). Ca(II) dissociation is proposed to occur in the vertical direction along the shortest path to solvent (boldface arrow) after the steric block of the coordinating axial side chain is removed by a conformational change.

Characterization of the Engineered Ca(II) Sites. The engineered galactose binding proteins exhibited no detectable structural or functional perturbations outside the Ca(II) site, as determined by measurements of D-glucose affinity and NMR chemical shifts (31). The wild-type site is highly specific for Ca(II), effectively excluding the physiological Na(I), K(I), and Mg(II) ions (35, 36). However, as typically observed for EF-hand sites, certain other metal cations, including the trivalent lanthanides, can replace Ca(II).

Tb(III), a fluorescent lanthanide, was the metal of choice for kinetic studies because each of the engineered sites exhibited Tb(III) affinities and dissociation kinetics in measurable ranges; in addition, bound Tb(III) can be monitored by a sensitive fluorescence energy transfer assay. [In contrast, Ca(II) dissociation kinetics could not be measured because fluorescent Ca(II) indicators were observed to perturb protein folding (data not shown).] The effective ionic radius of Tb(III) is similar to that of Ca(II) (0.98 and 1.06 Å for sevenfold coordination, respectively), and it yields the same coordination in EF-hand sites. Thus, Tb(III) can substitute for Ca(II) in EF-hand site activation (37–39). It is worth noting, however, that electrostatic effects may be exaggerated for the trivalent substrate Tb(III) relative to Ca(II).

In the present case, Tb(III) dissociation time-course experiments were triggered by addition of 0.3 mM EDTA, which was nonperturbing since EDTA concentrations up to 3 mM yielded identical Tb(III) dissociation kinetics. Subsequently, the bound Tb(III) population, which decreased as the Tb(III) dissociated and was trapped by the chelator, was continuously quantitated by steady-state nonradiative energy transfer from Trp-127 to the bound Tb(III) ion (40). In the case where dissociation was sufficiently fast ($k_{off} > 1$ sec^{-1}), the time course was determined by stopped-flow fluorescence.

Tb(III) Dissociation Time Courses. The resulting time courses reveal dramatic differences between the kinetics of the four sites. The Tb(III) dissociation rate varies by more than four orders of magnitude, as summarized in Fig. 3 and Table 2. As predicted, for side chains with the same charge, the shorter side chain provides more rapid dissociation, yielding 110-fold and 24-fold rate increases for the Gln vs. Asn and the Glu vs. Asp pairings, respectively. For side chains of the same length, the acidic functionality generates slower Tb(III) dissociation, yielding 500-fold and 110-fold rate decreases for the Asn vs. Asp and the Gln vs. Glu pairings, respectively. Thus the results indicate that the kinetic tuning model correctly predicts the sign of changes in metal ion dissociation rates resulting from both steric and electrostatic modifications of the axial side chain at the ninth loop position.

A key question is whether dissociation kinetics can be tuned independently from metal ion affinity. This question was addressed by comparing the dissociation rates and metal ion affinities of the four sites, as summarized in Table 2. No correlations between dissociation and affinity were ob-

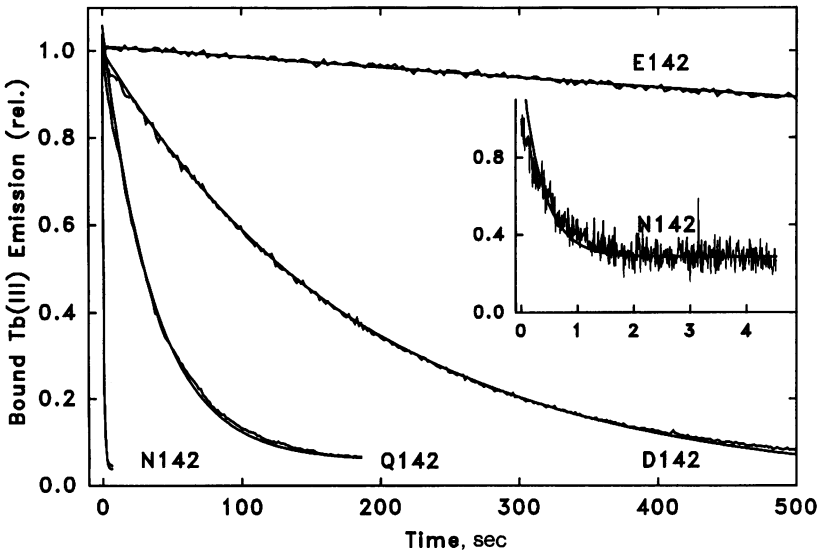

FIG. 3. Time courses of Tb(III) dissociation from the engineered EF-hand model site. Illustrated are the Tb(III) dissociation reactions of four versions of the model EF-hand site; the wild-type site, which possesses Gln-142 at the ninth EF-loop position, and three engineered sites possessing Glu, Asn, and Asp at this position. (*Inset*) Additional stopped-flow data for the Asn-142 site. Time courses were modeled by a single decaying exponential, representing first-order dissociation from a homogeneous population of sites. The resulting nonlinear least squares best fit curves are shown overlayed on the data. Tb(III) k_{off} values are summarized in Table 2. Samples contained 2.5 μM protein, 25 μM $TbCl_3$, 10 mM Pipes·KOH (pH 6.0), and 100 mM KCl. Dissociation reactions at 25°C were triggered by the addition of 0.3 mM EDTA. rel., Relative.

served: the Asn-142 and Asp-142 sites exhibit indistinguishable Tb(III) affinities (31), but dissociation is 500-fold more rapid from the former site; the Tb(III) affinity of the Gln-142 site is 1.9-fold greater than the Glu-142 site (31), but dissociation from the former is 110-fold faster. Perhaps the most surprising observation is that the Asn-142 site, which exhibits the highest Tb(III) affinity, also yields the fastest Tb(III) dissociation. At the same time, the Glu-142 site, which exhibits the lowest Tb(III) affinity, provides the slowest Tb(III) dissociation, fully 1.2×10^4-fold slower than the Asn-142 site. Thus, the unique structure of the EF-hand site enables its Tb(III) dissociation kinetics to be significantly altered without a corresponding change in its metal ion affinity.

Ionic Strength and Temperature Dependence of Ion Dissociation Rates. The ionic strength dependence of Tb(III) dissociation is summarized in Table 2 for each site. Overall the ionic strength dependence is 4- to 10-fold lower than expected for the dissociation of a solvent-exposed +3 ion from a −3 site [for which the predicted (41) dependence is $(z_1z_2)^{1/2} = 3$; compare with Table 2]. Finally, Table 2 also reveals a correlation between the dissociation rates and the observed Arrhenius activation free enthalpies.

Table 2. Equilibrium and kinetic parameters of Tb(III) dissociation from the engineered EF-hand model site

Site	K_d, μM	k_{off}, s^{-1} ($\times 10^3$)	$(z_1z_2)^{1/2}$, *e*	ΔH_{Arr}, kcal/mol
Q142E	280 ± 90	0.10 ± 0.02	0.3	12 ± 1
Q142D	50 ± 10	2.4 ± 0.1	0.8	11 ± 1
Q142(WT)	150 ± 50	11 ± 1	0.7	10 ± 1
Q142N	50 ± 20	1200 ± 100	0.7	4 ± 1

Shown are the parameters of the wild-type site (Q142) and three sites engineered at the ninth EF-loop position (Q142E, Q142D, and Q142N). K_d is the previously measured equilibrium Tb(III) dissociation constant at 25°C (31). k_{off} is the rate constant for Tb(III) dissociation at 25°C. The sites are listed in increasing order of this parameter. $(z_1z_2)^{1/2}$ is the ionic strength dependence of the Tb(III) dissociation rate at 25°C, measured by varying the KCl concentration from 25 to 400 mM. The resulting rates were best fit to the equation derived for ionic dissociation in solution, $\ln(k_{off}) = \ln(k_0) + 2.3(z_1z_2)\mu^{1/2}$, where μ is the ionic strength, k_0 is the dissociation rate constant at zero ionic strength, and z_1z_2 is the product of the dissociating charges (41). ΔH_{Arr} is the Arrhenius activation energy of the dissociation rate, measured over the range 15–35°C (1 cal = 4.184 J).

DISCUSSION

The Tb(III) dissociation rates of the wild-type (Q142) and engineered (Q142N, Q142D, and Q142E) sites suggest that the ninth position of the EF-hand loop plays a major role in tuning metal dissociation kinetics (Figs. 1 and 2 and Table 1). Side chains that provide direct coordination at this position (Gln or Glu) yield dissociation rates one to two orders of magnitude slower than shorter side chains; whereas a negatively charged side chain (Glu or Asp) slows dissociation by two to three orders of magnitude relative to the corresponding neutral side chain. Moreover, these kinetics can be varied independently of affinity, indicating that side-chain substitutions can tune the barrier height of the dissociative transition state while leaving the stability of the ion site complex unchanged relative to the empty site. This remarkable property is predicted to provide an important physiological advantage: the dissociation rate of a given EF-hand site, which in part determines the inactivation kinetics of the Ca(II) signal, can be tuned as required for optimal pathway timing, while the Ca(II) affinity can be independently optimized to match the Ca(II) concentration during an activation flux. The observed insensitivity of metal ion affinity to substitutions at the ninth loop position warrants further examination: a molecular understanding of this insensitivity would be facilitated by additional structural information regarding the empty and Tb(III)-occupied sites.

The ionic strength and temperature dependence of the Tb(III) dissociation rates reveal additional features of the dissociative transition state. For each site, the relatively weak ionic strength dependence of the dissociation rate suggests that the ionic transition state is partially buried within the protein where it is shielded from solvent. Alternatively, the effective charge of the site during the transition state may be reduced by protonation of multiple coordinating carboxylates. If simple transition state theory describes the dissociation, then the temperature dependence reveals a

strong correlation between the Arrhenius activation enthalpy and the dissociation rate but does not quantitatively account for the observed rates, indicating that entropic factors also contribute. Solvent reorganization around the Ca(II) binding loop could provide one such entropic factor.

Additional structural features of the EF-hand site are expected to contribute to kinetic tuning, including the composition of other loop positions and the binding of Ca(II) or protein ligands at allosterically coupled sites. However in specific cases (for example, the parvalbumin family, which exhibits a perfectly conserved Glu at the ninth loop position of the N-terminal site and which binds no protein ligands), the side chain at this position is proposed to be a critical one in the kinetic control of Ca(II) signaling.

This work was supported by a National Institutes of Health grant to J.J.F. (GM48203); M.R. was sponsored by the Feodor-Lynen Postdoctoral Fellowship of the Alexander v. Humboldt Foundation, Bonn, Germany.

1. Nakayama, S., Moncrief, N. D. & Kretsinger, R. H. (1992) *J. Mol. Evol.* **34,** 416–448.
2. Baimbridge, K. G., Celio, M. R. & Rogers, J. H. (1992) *Trends Neurosci.* **15,** 303–308.
3. Grabarek, Z., Tao, T. & Gergely, J. (1992) *J. Muscle Res. Cell Motil.* **13,** 383–393.
4. Hanson, P. I. & Schulman, H. (1992) *Annu. Rev. Biochem.* **61,** 559–601.
5. Onek, L. A. & Smith, R. J. (1992) *J. Gen. Microbiol.* **138,** 1039–1049.
6. Roberts, D. M. & Harmon, A. C. (1992) *Annu. Rev. Plant Physiol. Plant Mol. Biol.* **43,** 375–414.
7. Marsden, B. J., Shaw, G. S. & Sykes, B. D. (1990) *Biochem. Cell. Biol.* **68,** 587–601.
8. Strynadka, N. C. J. & James, M. N. G. (1989) *Annu. Rev. Biochem.* **58,** 951–998.
9. Ahmed, F. R., Przybylska, M., Rose, D. R., Birnbaum, G. I., Pippy, M. E. & MacManus, J. P. (1990) *J. Mol. Biol.* **216,** 127–140.
10. Declercq, J.-P., Tinant, B., Parello, J. & Rambaud, J. (1991) *J. Mol. Biol.* **220,** 1017–1039.
11. Taylor, D. A., Sack, J. S., Maune, J. F., Beckingham, K. & Quiocho, F. A. (1991) *J. Biol. Chem.* **266,** 21375–21380.
12. Roquet, F., Declercq, J.-P., Tinant, B., Rambaud, J. & Parello, J. (1992) *J. Mol. Biol.* **223,** 705–720.
13. Meador, W. E., Means, A. R. & Quiocho, F. A. (1992) *Science* **257,** 1251–1255.
14. Davis, T. N., Urdea, M. S., Masiarz, F. R. & Thorner, J. (1986) *Cell* **47,** 423–431.
15. Geiser, J. R., Vantuinen, D., Brockerhoff, S. E., Neff, M. M. & Davis, T. N. (1991) *Cell* **65,** 949–959.
16. Herzberg, O. & James, M. N. G. (1985) *Biochemistry* **24,** 5298–5302.
17. Vyas, N. K., Vyas, M. N. & Quiocho, F. A. (1987) *Nature (London)* **327,** 635–638.
18. Swain, A. (1988) Ph.D. thesis (Univ. of South Carolina, Columbia).
19. Babu, Y. S., Bugg, C. E. & Cook, W. J. (1988) *J. Mol. Biol.* **203,** 191–204.
20. Herzberg, O. & James, M. N. G. (1988) *J. Mol. Biol.* **203,** 761–769.
21. Pechere, J.-F., Derancourt, J. & Haiech, J. (1977) *FEBS Lett.* **75,** 111–114.
22. Hou, T.-T., Johnson, J. D. & Rall, J. A. (1992) *J. Physiol. (London)* **449,** 399–410.
23. Potter, J. D. & Johnson, J. D. (1982) in *Calcium and Cell Function*, ed. Cheung, W. (Academic, New York), Vol. 2, pp. 145–173.
24. Ashley, C. C., Mulligan, I. P. & Lea, T. J. (1991) *Q. Rev. Biophys.* **24,** 1–73.
25. Breen, P. J., Johnson, K. A. & Horrocks, W. D., Jr. (1985) *Biochemistry* **24,** 4997–5004.
26. Potter, J. D., Johnson, J. D., Dedman, F. R., Schreiber, W. E., Mandel, F., Jackson, R. L. & Means, A. R. (1977) in *Calcium Binding Proteins and Calcium Function*, eds. Wasserman, R. G., Corradin, R. A., Carafoli, E., Cretsinger, R. H., Maclennan, D. H. & Siegel, F. L. (North-Holland, New York), pp. 239–250.
27. Sekharudu, Y. C. & Sundaralingam, M. (1988) *Protein Eng.* **2,** 139–146.
28. Cavé, A., Daurer, M. F., Parello, J., Saint-Yves, A. & Sempéré, R. (1979) *Biochimie* **61,** 755–765.
29. Corson, D. C., Williams, T. C. & Sykes, B. D. (1983) *Biochemistry* **22,** 5882–5889.
30. Chao, S. H., Suzuki, Y., Zysk, J. R. & Cheung, W. Y. (1984) *Mol. Pharmacol.* **26,** 75–82.
31. Falke, J. J., Snyder, E. E., Thatcher, K. C. & Voertler, C. S. (1991) *Biochemistry* **30,** 8690–8697.
32. Needham, J. V., Chen, T. Y. & Falke, J. J. (1993) *Biochemistry* **32,** 3363–3367.
33. Martin, S. R., Linse, S., Johansson, C., Bayley, P. M. & Forsén, S. (1990) *Biochemistry* **29,** 4188–4193.
34. Martin, S. R., Teleman, A. A., Bayley, P. M., Drakenberg, T. & Forsén, S. (1985) *Eur. J. Biochem.* **151,** 543–550.
35. Snyder, E. E., Buoscio, B. W. & Falke, J. J. (1990) *Biochemistry* **29,** 3937–3943.
36. Vyas, M. N., Jacobson, B. L. & Quiocho, F. A. (1989) *J. Biol. Chem.* **264,** 20817–20821.
37. Brittain, H. G., Richardson, F. S. & Martin, R. B. (1976) *J. Am. Chem. Soc.* **98,** 8255–8260.
38. Horrocks, W. D. & Albin, M. (1984) *Prog. Inorg. Chem.* **31,** 1–104.
39. Moews, P. C. & Kretsinger, R. H. (1975) *J. Mol. Biol.* **91,** 229–232.
40. Careaga, C. L. & Falke, J. J. (1992) *J. Mol. Biol.* **226,** 1219–1235.
41. Glasstone, S., Laidler, K. J. & Eyring, H. (1941) *The Theory of Rate Processes* (McGraw-Hill, New York).